Parametric Instability of a Liquid-Vapor Interface Close to the Critical Point

S. Fauve, K. Kumar, and C. Laroche
Laboratoire de Physique, Centre National de la Recherche Scientifique, Ecole Normale Supérieure de Lyon, 46 allée d'Italie, 69364 Lyon, France

D. Beysens
Service de Physique de l'Etat Condensé, Centre d'Etudes de Saclay, 91191 Gif sur Yvette, France

Y. Garrabos
Laboratoire d'Ingénierie des Hautes Pressions, Centre National de la Recherche Scientifique, Université Paris-Nord, Avenue J. B. Clément, 93430 Villetaneuse, France
(Received 10 February 1992)

An experimental study of the parametric instability of a liquid-vapor interface close to the critical point is presented. A cell containing carbon dioxide at the critical density is vertically vibrated sinusoidally; the acceleration amplitude a_0 and the instability wavelength λ_0 at the instability onset are measured with respect to the excitation frequency and the critical temperature difference $T_c - T$. These measurements provide a simple way to determine the surface tension and the density difference between the two phases. When $T_c - T$ diminishes λ_0 decreases and reaches a finite value whereas a_0 diverges. The shape of the wave pattern appears to depend on $T_c - T$.

PACS numbers: 47.20.−k, 64.70.Fx

The generation of surface waves by vertically vibrating a horizontal fluid layer has been known since Faraday [1]. However, most of the experimental studies consisted of vibrating a liquid layer with a free surface under air at atmospheric pressure [2]. We present here a similar study, but with a liquid layer surrounded by its vapor in a closed container, and we report the instability behavior when the experiment is performed closer and closer to the liquid-vapor (L-V) critical point. The response of the L-V interface to a parametric excitation is thus observed in the vicinity of the critical point, at which the interface disappears. We show that the measurements of the instability wavelength λ_0 and of the critical acceleration a_0 at the instability onset determine important characteristics of the L-V interface, i.e., the capillary length l_c and the relative density difference $(\rho_l - \rho_v)/(\rho_l + \rho_v)$ between the two phases. In addition, new phenomena are seen to occur very close to the critical point, roughly for $T_c - T < 0.02$ K. First, the instability wavelength saturates at a finite value, although l_c vanishes for $T \to T_c$. Second, the selected wave pattern above the instability onset changes from squares, as observed in previous experiments with fluids in contact with air at atmospheric pressure, to a one-dimensional standing-wave pattern. As the acceleration is increased further, these patterns display a transition to spatiotemporal chaos by nucleating defects.

The fluid container is a cylindrical cell with axis perpendicular to gravity, 10 mm in diameter and 6.5 mm in height. The upper and lower boundaries are made of transparent sapphire windows which enable the patterns to be observed. The cell is filled with carbon dioxide to a density ρ within $\pm 0.2\%$ of the critical density ρ_c, and is maintained in a water bath thermally regulated to less than ± 0.5 mK of a set temperature T in the range $0 < T_c - T < 1$ K (for CO_2, $T_c = 304.13$ K). Temperature is measured with a HP 2804A quartz thermometer (10^{-4} K resolution). The cell is vertically vibrated with the help of a BK 4809 vibration exciter driven with a HP 8904A frequency synthesizer in the frequency range $40 < f < 135$ Hz (frequency precision better than 10^{-6}). The amplitude a of the sinusoidal acceleration, which is the relevant bifurcation parameter, is measured with an accelerometer BK 4375. The L-V interface is visualized with a vertical light beam crossing the container, generated by a stroboscope synchronized at the surface-wave frequency, i.e., half the external driving frequency f. Two photographs of the wave pattern above the instability onset are displayed in Fig. 1 for two temperatures. Far from T_c, a square pattern is observed [Fig. 1(a)]; for $T_c - T \leq 0.02$ K, the pattern takes the form of parallel lines [Fig. 1(b)]. Depending on $T_c - T$ the pattern thus consists of either a one-dimensional standing wave or two standing waves with wave vectors at a right angle.

The experiments are conducted by increasing the acceleration amplitude a at a fixed value of f, and at a given $T_c - T$. For a critical value $a_0(f, T_c - T)$ of a, the flat L-V interface becomes unstable and a standing wave bifurcates supercritically; i.e., the transition from the flat interface to the wave pattern involves no hysteresis. Its wavelength at onset, $\lambda_0(f, T_c - T)$ is plotted in Fig. 2 as a function of f for two different values of $T_c - T$.

The simplest way to model this instability is to consider the liquid and its vapor as two layers of incompressible fluids, and then to take into account viscous losses in a perturbative way. Assuming periodic lateral boundary conditions, a linear analysis [3] shows that the amplitude of an eigenmode of the interface with wave number k obeys a Mathieu equation, with an eigenfrequency $\omega(k)$

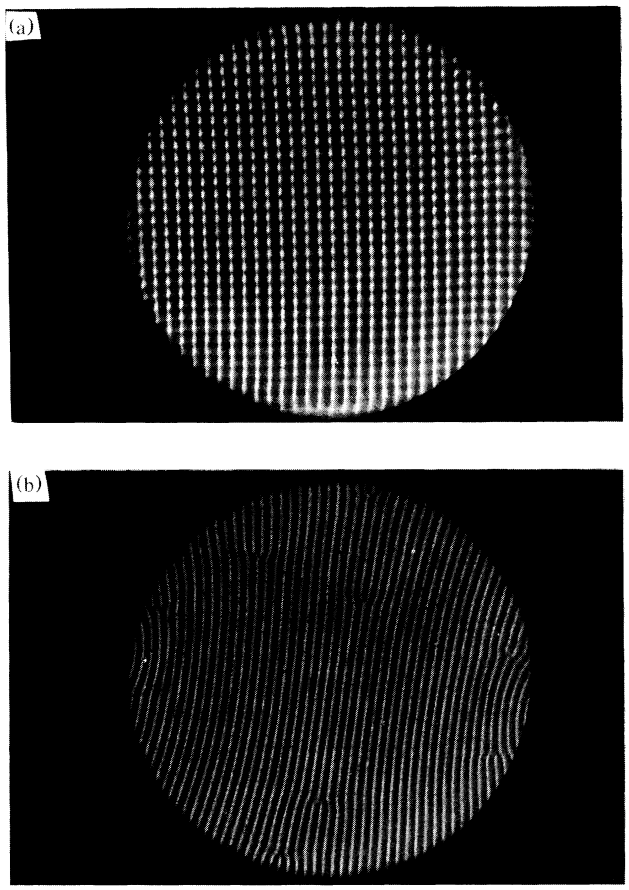

FIG. 1. Parametrically generated wave patterns: (a) $f=60$ Hz, $T_c-T=0.08$ K; (b) $f=60$ Hz, $T_c-T=0.02$ K.

at the onset:

$$\omega^2(k)=\frac{(\rho_l-\rho_v)gk+\sigma k^3}{\rho_l+\rho_v}, \tag{1}$$

where ρ_l and ρ_v are the densities of the liquid and vapor phases, g is the acceleration due to gravity, and σ is the interfacial surface tension (the correction due to the finite heights of the layers is negligible in our experiments) [3]. Such a linear analysis predicts the parametric amplification of a standing wave with wave number k as

$$\omega(k)=\pi f. \tag{2}$$

This parametric-resonance condition is satisfied only approximately in a finite-size container because of the wave-number quantization due to lateral boundary conditions. In a large enough container, higher-frequency resonances of the Mathieu equation are never observed because they are more strongly damped by viscous dissipation. The critical acceleration amplitude for instability onset can be roughly estimated by assuming only viscous dissipation in the bulk [3],

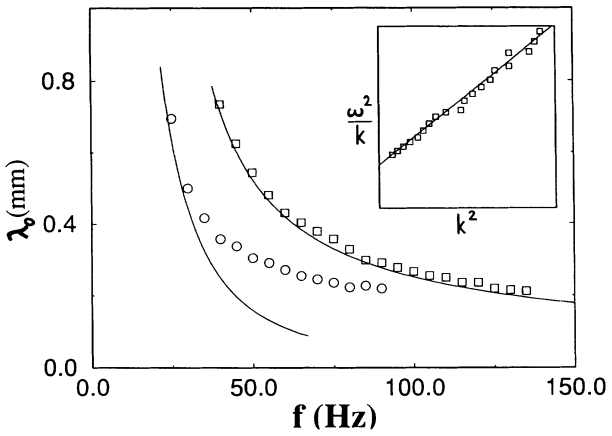

FIG. 2. Wavelength λ_0 at instability onset as a function of the excitation frequency f for different values of T_c-T; $T_c-T=0.078$ K (□) and $T_c-T=0.007$ K (○). Theoretical prediction using the dispersion relation (1) (solid lines). Inset: ω^2/k as a function of k^2 for $T_c-T=0.078$ K.

$$a_0\approx 8\pi f k(\nu_l+\nu_v)\frac{\rho_l+\rho_v}{\rho_l-\rho_v}, \tag{3}$$

where ν_l and ν_v are the kinematic viscosities of the liquid and vapor phases.

Using Eqs. (1) and (2), one determines the relative density difference, $(\rho_l-\rho_v)/(\rho_l+\rho_v)$, and the capillary length, $l_c=[\sigma/(\rho_l-\rho_v)g]^{1/2}$, of the L-V system, from the measurement of the wavelength and the frequency at the instability onset. As expected from Eq. (1), $\omega^2(k)/k$ as a function of k^2 is a straight line as displayed in the inset in Fig. 2 for $T_c-T=0.078$ K. The corresponding relative density difference and the capillary length are obtained from the slope and the intercept. This linear relation is not observed for very small T_c-T, e.g., for the Fig. 2 data at $T_c-T=0.007$ K. This means that the simple model above is not valid very close to the critical point. This is also shown clearly in Fig. 3 where λ_0 is plotted as

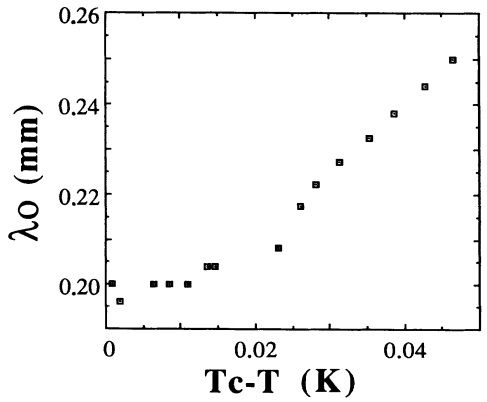

FIG. 3. Wavelength λ_0 at instability onset as a function of T_c-T for an excitation frequency $f=70$ Hz.

a function of $T_c - T$ for $f = 70$ Hz. One observes that λ_0 saturates at a finite value λ_S when $T \to T_c$, in contrast to Eqs. (1) and (2) which predict that $\lambda_0 \to 0$. In Eq. (1), both $\rho_l - \rho_v$ and σ vanish at T_c, whereas ω is constant; thus $k \to \infty$, or $\lambda_0 \to 0$. The value of $T_c - T$ for which λ_0 saturates decreases for decreasing excitation frequency f; roughly 0.02 K at 70 Hz, it becomes too small to be measured for $f < 50$ Hz. Note that the measurements at $T_c - T = 0.078$ K in Fig. 2 all correspond to nonsaturated λ_0.

Apart from the fact that gravity stratification may affect the behavior of σ and $\rho_l - \rho_v$, the main deficiency of our model in the vicinity of the critical point is that it neglects dissipation to leading order. Dissipation, due to the viscous fluid flow generated in the bulk of the gas and liquid layers by the interface instability, scales like $(\nu_l + \nu_v)k^2$. This cannot be considered as a perturbation in the vicinity of the critical point where k becomes large, as is qualitatively shown by the wavelength-frequency curves of Fig. 2: For $T_c - T = 0.078$ K, the model (solid line) fits the data over the entire wave-number range; for smaller $T_c - T$, e.g., $T_c - T = 0.007$ K, agreement is observed only at small wave numbers. A correct analysis would require the resolution of the Floquet problem that can be avoided in the weakly dissipative model considered above. To our knowledge, this has not been performed so far, even for any other parametrically amplified wave problem. The saturation of the wavelength to a finite value when $T \to T_c$ (Fig. 3) can also be understood as a viscous cutoff length λ_S, for which the surface wave is too strongly damped to be parametrically amplified. It can be checked that $[(\nu_l + \nu_v)/f]^{1/2}$ gives the right order of magnitude for λ_S, which scales as $1/\sqrt{f}$ when the excitation frequency is varied.

When using Eq. (1) in the $T_c - T$ range where it is approximately correct, numerical values for $(\rho_l - \rho_v)/(\rho_l + \rho_v)$ and l_c are found to be about 5% to 10% higher for the former and about 15% to 20% higher for the latter than those reported in the literature [4]. Experimental errors can be found due to the wavelength quantization by the lateral boundary conditions. The pattern typically involves 20 to 50 wavelengths, so the experimental error is less than 5%. We think therefore that the main part of the error is due to the use of Eq. (1) that neglects dissipation.

For $T_c - T$ fixed, the critical acceleration for the instability onset increases as a function of the frequency. We have checked that the rough estimation of Eq. (3) predicts the correct order of magnitude. It is more interesting to consider the behavior of a_0 as $T \to T_c$. This is displayed in Fig. 4 for different values of f. We have plotted here a_0/fk (k is the pattern wave number at onset) as a function of $1 - T/T_c$. Qualitatively, the divergence of a_0 as $T \to T_c$ is due to the vanishing density difference and to the increasing dissipation as smaller wavelengths are involved. This is clearly observed from our data. Quantitatively, according to Eq. (3), a_0/fk should scale like $(\rho_l - \rho_v)^{-1}$, i.e., as $(T_c - T)^{-\beta}$ with $\beta = 0.325$ the critical exponent, since $\nu_l + \nu_v$ and $\rho_l + \rho_v$ are nearly constant. Figure 4 shows the limited validity of Eq. (3). First, the data at different frequencies only collapse roughly to a single curve. Second, slight distorsions to the power-law behavior are observed.

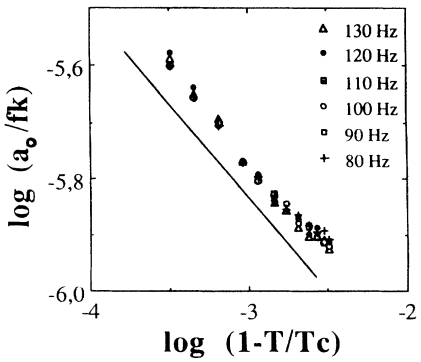

FIG. 4. Divergence of the critical acceleration a_0 for instability onset, with respect to $T \to T_c$ and for different excitation frequencies f. k is the pattern wave number at instability onset. The solid line is of slope $\beta = 0.325$ as predicted by Eq. (3).

A linear stability analysis accurately taking into account dissipation would be of great interest, since the dispersion curve could then be used as a simple method to measure surface tension, even very close to the critical point. The critical acceleration data could be used also to determine the density difference and to measure dissipation in the vicinity of the critical point. Note, however, that the hydrodynamic instability and the critical phenomena are quite entangled. For instance, one expects L-V mixing or phase change at the interface to act as an additional dissipation. Compressible effects might also become important close to the critical point. This might limit the validity of our measurement technique very close to the critical point except if all these phenomena are taken into account in the theoretical analysis.

Above a_0 the instability saturates in a nonlinear way and generates a stationary standing-wave pattern. The bifurcation is supercritical. From previous experimental observations, it is usually believed that the Faraday instability generates square patterns in large-aspect-ratio containers where boundary effects are considered to be negligible. This has been recently shown analytically [5]. We show here that, instead, the selected pattern strongly depends on the fluid parameters. Far from T_c, a square pattern is observed [Fig. 1(a)]. It consists of the superposition of two standing waves with wave vectors at a right angle. Close to T_c, the stable selected pattern is a one-dimensional standing wave [Fig. 1(b)]. The transition takes place roughly at $T_c - T = 0.02$ K. This value slightly decreases with increasing frequency, but this dependence is too small to be quantified. Note that the square-to-roll transition does not occur concomitantly

with the saturation of the wavelength (except for $f \approx 70$ Hz). Slight boundary effects that locally bend the patterns can be seen in the Fig. 1 photographs, but we have observed that the pattern orientation varies from one experiment to the other. There is no contradiction, however, between our experiment and the analysis of Ref. [5] which was performed in the limit where capillarity is the dominant term in the dispersion relation, and assuming negligible dissipation. In the vicinity of the critical point, surface tension vanishes faster than the third power of the density difference. Thus the gravity term is still the dominant one even though the wavelength is becoming very small. Moreover, as shown above, dissipation cannot be taken into account as a small perturbation. It has been very recently observed that a pattern with parallel lines can be also obtained with ordinary liquids in the capillary-wave regime if the dissipation is large enough [6].

As the vibration is increased further, these wave patterns display a transition to spatiotemporal chaos via erratic nucleation of defects, as is very often observed in pattern-forming instabilities. Some of these defects are already apparent in Fig. 1(b).

We have presented in this Letter a first step in the study of the interaction between an instability and a phase transition. We expect to improve our temperature stability in order to perform experiments closer to the critical point, but as pointed out above, theoretical analysis should also be done in order to answer open questions about the quantitative effects of dissipation, L-V mass transfers, and compressibility. More generally, we expect interesting new phenomena from the interaction between the interface instability and the L-V phase transition. This is because the relevant microscopic length scale of the problem, i.e., the interface thickness, increases (at least until gravity affects the process) whereas the macroscopic length scale, i.e., the instability wavelength, decreases near the transition. Consequently, both the instability and the phase transition might therefore be strongly affected by their coupling which increases near the critical point.

We thank S. Edwards for useful discussions and A. Wilkinson for a critical reading of the manuscript. This work has been supported by the CNES (Centre National d'Etudes Spatiales) under Contracts No. 90/254 and No. 91/277.

[1] M. Faraday, Philos. Trans. R. Soc. London **52**, 299 (1831).

[2] Recent experiments on the Faraday instability in large-aspect-ratio containers have been performed by R. Keolian, L. A. Turkevich, S. J. Putterman, I. Rudnick, and J. A. Rudnick, Phys. Rev. Lett. **47**, 1133 (1981); A. B. Ezerskii, P. I. Korotin, and M. I. Rabinovich, Pis'ma Zh. Eksp. Teor. Fiz. **41**, 129 (1985) [JETP Lett. **41**, 157 (1985)]; N. Trufillaro, R. Ramshankar, and J. P. Gollub, Phys. Rev. Lett. **62**, 422 (1989); S. Ciliberto, S. Douady, and S. Fauve, Europhys. Lett. **15**, 23 (1991).

[3] This linear analysis is similar to that used for a vertically vibrated liquid layer under air at atmospheric pressure: T. B. Benjamin and F. Ursell, Proc. R. Soc. London A **225**, 505 (1954); K. Kumar (to be published).

[4] See, for instance, R. M. Moldover, Phys. Rev. A **31**, 1022 (1985), and references therein.

[5] S. T. Milner, J. Fluid Mech. **225**, 81 (1991).

[6] S. Edwards (private communication).

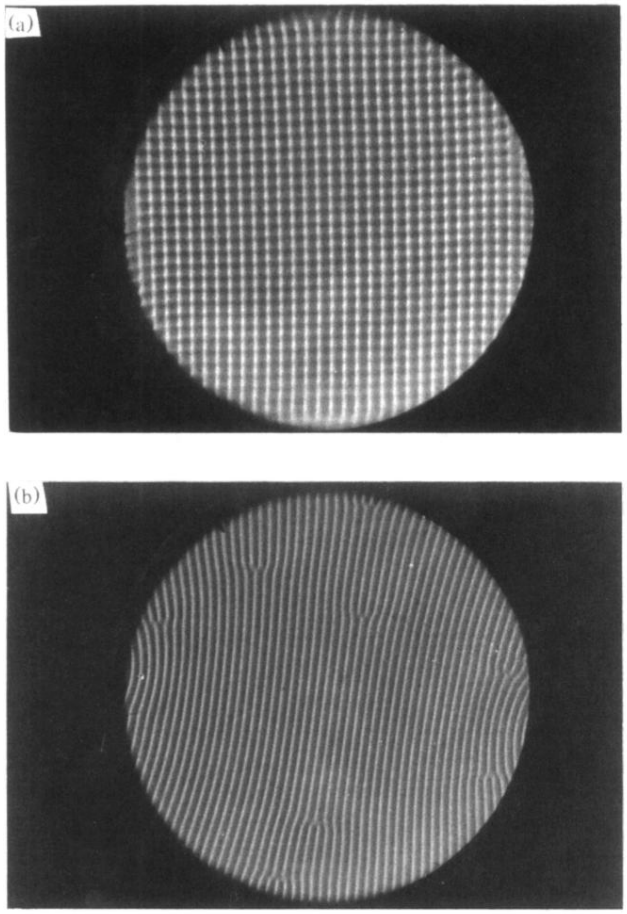

FIG. 1. Parametrically generated wave patterns: (a) $f=60$ Hz, $T_c - T = 0.08$ K; (b) $f=60$ Hz, $T_c - T = 0.02$ K.